IEEE Access
Multidisciplinary ⁝ Rapid Review ⁝ Open Access Journal

Received September 30, 2020, accepted October 22, 2020, date of publication October 29, 2020,
date of current version November 13, 2020.

Digital Object Identifier 10.1109/ACCESS.2020.3034743

ISAR Imaging of Multiple Targets With Time-Delay Receive Array

MENGDI ZHANG[1], GUISHENG LIAO[1], (Senior Member, IEEE), JINGWEI XU[1], (Member, IEEE), LAN LAN[1], (Member, IEEE), AND KA DENG[2]

[1]National Laboratory of Radar Signal Processing, Xidian University, Xi'an 710071, China
[2]Institute of Biomedical and Health Engineering, Shenzhen Institutes of Advanced Technology, Chinese Academy of Sciences, Shenzhen 518055, China

Corresponding authors: Mengdi Zhang (zhangmengdi8101@163.com) and Jingwei Xu (xujingwei1987@163.com)

This work was supported in part by the National Nature Science Foundation of China under Grants 61931016, 62071344, 61911530246.

ABSTRACT For inverse synthetic aperture radar (ISAR), it is desirable to perform simultaneously imaging of multi-target within a wide spatial angle region. Besides, it is likely that multiple targets are covered by several beams, or sometimes within a single beam, which results in imaging challenge for each single target. To alleviate this problem, this paper devises a new approach by introducing time delay across different receive array elements, realizing multi-target separation and independent imaging. By using the time-delay receive array with linear frequency modulation (LFM) waveform, the equivalent receive beampattern is range-angle-dependent and it is possible to perform beamforming in joint range and angle domain. In the time-delay receive array, an element compensation method is presented to cope with the variation of the equivalent spatial frequency. After receive beamforming, the conventional high resolution ISAR imaging method can be performed. With the proposed method, the multi-target echo can be separated under low signal noise ratio (SNR). Simulation results have verified the effectiveness of the proposed approach.

INDEX TERMS Multi-target, time-delay receive array, inverse synthetic aperture radar (ISAR), receive beamforming.

I. INTRODUCTION

Inverse synthetic aperture radar (ISAR) plays an important role in radar applications. In the ISAR system, multiple targets imaging and recognition is a significant issue with the development of group aircrafts or unmanned aerial vehicles [1], [2]. It is known that ISAR target is non-cooperative, whereas the target motion usually includes two components, namely translation and rotation. The translation will lead to the range-bin shift and phase distortion. As a result, motion compensation is a principal step in ISAR imaging. There are many techniques to handle the motion compensation issue in existing literatures [3], [4]. In multi-target situation, the compensation performance may compromise due to cross influence among these targets, resulting in image blurring in the end. On one hand, when multiple targets are located in the mainbeam, the echo of each target cannot be separated from range or azimuth. On the other hand, due to the diversity of translational motion of each target, the motion compensation for one target is not effective for other targets, namely, the motion compensation for each target cannot be realized simultaneously.

Generally, there are two catalogs of ISAR imaging methods for multi-target. The first catalog uses straightforward approach for the single target to cope with ISAR imaging of multi-target. In this situation, multiple targets are treated as a whole rigid body to carry out unified motion compensation [5]–[9]. Then the signal is processed by time-frequency transform. Thus this method results in cross-term and low-resolution problems for multi-target. The second catalog tries to separate these multiple targets and perform ISAR imaging individually. The second catalog is based on separation of the echoes [10]–[13], which can be divided into two types. In the first type, the signals can be separated by different motion parameters. In the second type, the signals are separated in the bulk image. However, these two types produce a heavy computational burden.

Time-delay receive array is capable of forming angle-range-dependent beampattern, which is also explored in frequency diversity array (FDA). However, these two schemes are different because i) time-delay receive array uses different time delays among array elements while FDA employs different frequency among array elements. ii) Time-delay receive array realizes time-delay diversity in the receive port while FDA implements frequency diversity in the transmit port. FDA was first introduced by Antonik in 2006, which has attracted growing attention in recent years [14], [15]. The characteristics of angle-range-dependent beampatterns for FDA are introduced in [16], [17]. The combination of FDA with MIMO technology can provide larger DOFs, which

The associate editor coordinating the review of this manuscript and approving it for publication was Guolong Cui.

has drawn considerable attention [18]. In [19], the range-angle-dependent characteristic of FDA-MIMO radar is properly utilized and an unambiguous range and angle estimation method is proposed. Further exploration of frequency diverse array in MIMO radar to improve the range ambiguous clutter suppression performance is suggested in [20], [21]. In [22], a novel FDA-SAR system is studied for HRWS imaging in the presence of range ambiguity within the swath. FDA has been widely used in recent years. However, the time-delay receive array has not been studied in the literature. The time-delay receive array introduces different time delays among array elements, thus resulting in multi-rate sampling of receive signal.

In ISAR system, there is an urgent requirement for simultaneously imaging of multiple targets, which may be located in a wide angle region covered by several beams. In this situation, it is difficult to realize simultaneously imaging of these multiple targets with the conventional radar, because each target requires a long dwelling time to obtain high resolution in azimuth. Thus, it usually becomes a trade-off between resolution ability and multi-target coverage. On the other hand, multiple targets can also be covered by a single beam, especially for the very-far field surveillance task. In such situation, the signal-to-noise ratio (SNR) is commonly very low for different targets after range compensation. Once there are multiple targets with the effective data raw, the imaging performance of each target will degrade due to cross influence for motion parameter estimation. If it is possible to separate these multiple targets in low SNR, the imaging performance can be improved, which is the motivation in this paper.

In this paper, we introduce the time-delay receive array and the corresponding ISAR multiple targets imaging framework. The multi-target imaging with time-delay receive array is implemented by exploiting the time-frequency relationship of LFM waveform. A multiple targets separation approach is proposed to realize multi-target independent imaging. Since the receive steering vector of time-delay receive array depends on both range and angle, the multi-target echoes are distinguishable in the equivalent spatial frequency domain. It is emphasized that the equivalent spatial frequency depends on the time-frequency relationship of LFM waveform and it is different from the conventional concept of spatial frequency. By utilizing the extra degrees-of-freedom (DOFs) in range and angle, it is capable of extracting the signal of desired section from multiple targets echo by performing receive beamforming in the equivalent spatial frequency domain. In the sequel, the traditional ISAR imaging method can be implemented to the reconstructed single-target echo. With the proposed method, the multi-target echoes can be separated simultaneously by applying multiple receive weight vectors corresponding to multiple targets. Besides, the desired target echo can be extract by the proposed method when the signal is drowned by noise due to low SNR.

The remaining sections are organized as follows. In section II, the signal model of the time-delay receive array is presented. In section III, an approach to separating these targets and imaging individually is proposed. In section IV, some simulations are presented to verify the effectiveness of the proposed method. In the section V, conclusions are drawn.

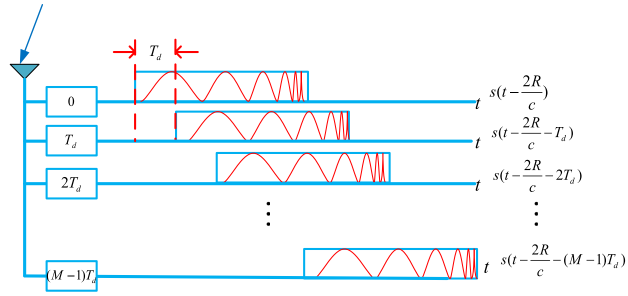

FIGURE 1. Time-delay LFM signal.

II. TIME-DELAY RECEIVE ARRAY

The time-delay receive array is introduced in this section. We first explore the principle of multi-sampling of LFM signal by assuming a single antenna, as shown in Figure.1. In the receiver, the signal is shifted by time delay $0, T_d, 2T_d, \ldots, (M-1)T_d$ respectively, which is referred to as multi-rate sampling. We assume a far-field point target at range R, and thus the baseband signal corresponding to time delay $(m-1)T_d$ is written as

$$x_m(t) = w\left[t - \frac{2R}{c} - (m-1)T_d\right] \exp\left(-j2\pi f_0 \frac{2R}{c}\right) \times \exp\left\{j\pi\mu\left[t - \frac{2R}{c} - (m-1)T_d\right]^2\right\} \quad (1)$$

where $w(t) = \begin{cases} 1, 0 \le t \le T_p \\ 0, else \end{cases}$. T_p is pulse duration. T_d is time-delay increment. f_0 is carrier frequency. μ is chirp rate. t is the fast time. Considering $(M-1)T_d < 1/B$, (1) can be approximately written as

$$x_m(t) \approx A\varphi(t)\alpha_m(t) \exp\left[j4\pi(m-1)\mu T_d \frac{R}{c}\right] \quad (2)$$

where $A = \exp(-4j\pi f_0 R/c)$ is the complex amplitude of the target. $\varphi(t)$ is the envelope of the signal.

$$\varphi(t) = w\left(t - \frac{2R}{c}\right) \exp\left[j\pi\mu\left(t - \frac{2R}{c}\right)^2\right] \quad (3)$$

$\alpha_m(t)$ can be expressed as

$$\alpha_m(t) = \exp\left[j\pi\mu(m-1)^2 T_d^2\right] \exp\left[-j2\pi(m-1)\mu T_d t\right] \quad (4)$$

As $\alpha_m(t)$ is dependent of system parameters, it can be compensated by constructing the compensation term corresponding to m-th sampling:

$$g_m(t) = \alpha_m^*(t) \quad (5)$$

Applying compensation, we have

$$\tilde{x}_m(t) = g_m(t)\, x_m(t) = A\varphi(t) \exp\left[j4\pi(m-1)\mu T_d \frac{R}{c}\right] \quad (6)$$

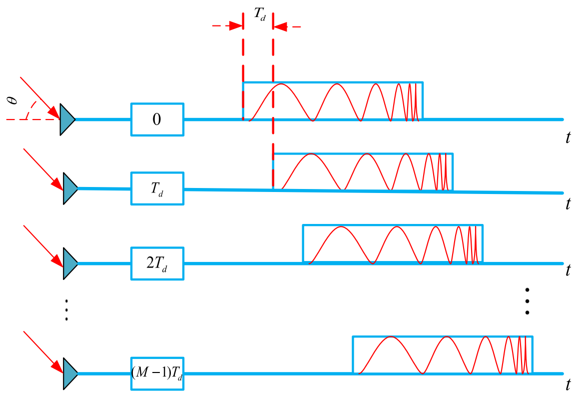

FIGURE 2. Time-delayed receive array.

By stacking all M samplings into a vector, it yields

$$\tilde{\mathbf{x}} = \left[\tilde{x}_1\ \tilde{x}_2 \cdots \tilde{x}_M\right]^T = A\varphi\,(t)\,\mathbf{a}\,(R) \tag{7}$$

where $\mathbf{a}\,(R)$ is expressed as

$$\mathbf{a}\,(R) = \begin{bmatrix} 1 & e^{j4\pi\mu T_d \frac{R}{c}} & \cdots & e^{j4\pi(M-1)\mu T_d \frac{R}{c}} \end{bmatrix}^T \tag{8}$$

Employing time delay of LFM signal with multi-sampling receiver, the range parameter is included in the steering vector of target, as shown in (7), which enables separation of target with different ranges. It is seen from (7) that the m-th entry of steering vector is written as

$$[\tilde{\mathbf{x}}]_m = A\varphi(t)e^{j4\pi(m-1)\mu T_d \frac{R}{c}} \tag{9}$$

Thus, the reconstructed signal has equivalent spatial frequency, which is written as

$$f_r = \frac{2\mu T_d R}{c} \tag{10}$$

It is seen that the multi-sampling strategy with a single antenna element introduces range parameter into the steering vector.

In the sequel, we further consider the uniform linear array (ULA) employed with the time delay at each receive array element as shown in Figure. 2 The array includes M receive elements. The time delay of the signal received by the m-th channel is expressed as

$$t_m = (m-1)T_d \tag{11}$$

Notice that m-th sampling and m-th array element is one-to-one in this framework. After introducing the time delay, the baseband signal received by the m-th channel is represented by

$$s_m = w\left[t - \tau_m - (m-1)T_d\right]\exp\left[-j2\pi f_0 \tau_m\right] \times \exp\left[j\pi\mu\left(t - \tau_m - (m-1)T_d\right)^2\right] \tag{12}$$

where τ_m is the time delay of target corresponding to the m-th element. For a far-field target located at angle θ and range R_0, we have

$$\tau_m = \frac{2R_0 - (m-1)d\sin(\theta)}{c} \tag{13}$$

Substituting (13) into (12), we have

$$s_m(t) = A_0\phi_m(t)\alpha_m(t)\exp\left[4j\pi\mu T_d\,(m-1)\,\frac{R_0}{c}\right] \times \exp\left[2j\pi\,(f_0 + (m-1)\mu T_d)\,\frac{(m-1)d\sin(\theta)}{c}\right] \tag{14}$$

where $A_0 = \exp(-4j\pi f_0 R_0/c)$ is the complex amplitude of the target. $\alpha_m(t)$ is independent of the target parameter and can be expressed as (4). $\phi_m(t)$ is the envelope of the signal.

$$\phi_m(t) = w\left[t - \frac{2R_0}{c} + \frac{(m-1)d\sin(\theta)}{c} - (m-1)T_d\right] \times \exp\left[j\pi\mu\left(t - \frac{2R_0}{c} + \frac{(m-1)d\sin(\theta)}{c}\right)^2\right] \tag{15}$$

In this work, we take the far-filed and narrowband array assumption. Moreover, it is assumed that $\mu T_d \ll f_0$ and $(M-1)T_d < 1/B$, which is usually reasonable in ISAR system. Thus, (14) can be approximately rewritten as

$$s_m(t) = A_0\phi(t)\alpha_m(t)\exp\left[4j\pi\mu T_d\,(m-1)\,\frac{R_0}{c}\right] \times \exp\left[2j\pi f_0\frac{(m-1)d\sin(\theta)}{c}\right] \tag{16}$$

where $\phi(t)$ is expressed as

$$\phi\,(t) = w\left(t - \frac{2R_0}{c}\right)\exp\left[j\pi\mu\left(t - \frac{2R_0}{c}\right)^2\right] \tag{17}$$

Similarly, with the compensation term $g_m(t)$, the target signal is obtained as

$$\tilde{\mathbf{s}} = \left[\tilde{s}_1\ \tilde{s}_2 \cdots \tilde{s}_M\right]^T = A_0\phi\,(t)\,\mathbf{a}\,(\theta, R_0) \tag{18}$$

where $\mathbf{a}\,(\theta, R_0)$ is expressed as

$$\mathbf{a}\,(\theta, R_0) = \begin{bmatrix} 1 \\ e^{j2\pi f_0\frac{d\sin(\theta)}{c} + j4\pi\mu T_d\frac{R_0}{c}} \\ \vdots \\ e^{\left(j2\pi f_0\frac{d\sin(\theta)}{c} + j4\pi\mu T_d\frac{R_0}{c}\right)(M-1)} \end{bmatrix} \tag{19}$$

where R_0 is the slant range between the target and the reference antenna. θ is the azimuth of the target. c is the speed of light. With exploration of time-frequency relationship of LFM waveform using the time-delay receive array, we obtain the equivalent spatial frequency as

$$f_{S,R} = f_r + f_\theta = \frac{2\mu T_d R}{c} + \frac{d}{\lambda}\sin\theta \tag{20}$$

Notice that the equivalent spatial frequency depends on the time-frequency relationship of LFM waveform and it is different from the conventional concept of spatial frequency.

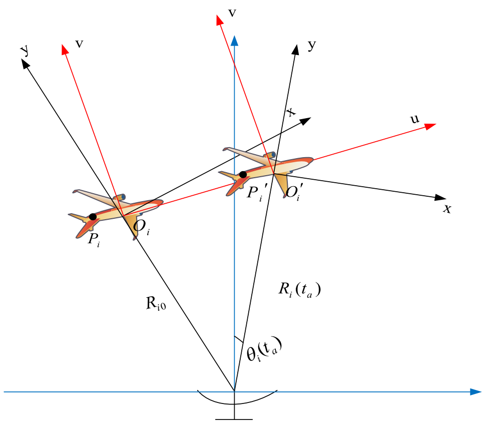

FIGURE 3. ISAR imaging geometry.

As the proposed time-delay receive array introduces range and angle parameters into the steering vector, it enables signal processing in joint range and angle domain.

III. MULTIPLE TARGETS IMAGING WITH TIME-DELAY RECEIVE ARRAY

A. MULTIPLE TARGETS ECHO

The ISAR imaging geometry is shown in Figure.3. Suppose the transmit antenna transmits a wide beam and there are multiple targets within the wide beam. The i-th target is rotating with respect to its geometry center point O_i with an angular velocity ω. $O-XY$ represents the reference coordinate system. During the azimuth time t_a, the platform center flies from O_i to O_i', while an arbitrary point scatter moves from $P_i(x_{ip0}, y_{ip0})$ to $P_i'(x_{ip}(t_a), y_{ip}(t_a))$.

Thus, the slant range between the radar and the point P_i is expressed as

$$R_{ip}(t_a) = \sqrt{(R_i(t_a) + y_{ip}(t_a))^2 + x_{ip}(t_a)^2} \tag{21}$$

where $R_i(t_a)$ is the instantaneous slant range between the radar and the point O_i. Using Taylor series approximation, we have

$$R_{ip}(t_a) \approx R_{i0} + v_{ri}t_a + y_{ip0} + x_{ip0}\omega t_a \tag{22}$$

where R_{i0} is the initial range between the i-th target and the radar. v_{ri} is the radial velocity of the i-th target. The multi-target echo received by m-th array element is expressed as

$$\begin{aligned} s_m(t, t_a) = &\sum_{i=1}^{I}\sum_{p=1}^{P} A_{ip}\alpha_m(t)\phi_{ip}(t) \\ &\times \exp\left[2j\pi f_0 \frac{(m-1)d\sin(\theta_i(t_a))}{c}\right] \\ &\times \exp\left[4j\pi\mu T_d(m-1)\frac{R_{ip}(t_a)}{c}\right] \end{aligned} \tag{23}$$

As aforementioned, since $\alpha_m(t)$ is dependent of the system parameters we can construct the compensation function as

$$h_m(t) = \exp\left[-j\pi\mu(m-1)^2 T_d^2\right]\exp\left[2j\pi(m-1)\mu T_d t\right] \tag{24}$$

Then, the signal after compensation is written as

$$\begin{aligned} &\tilde{s}_m(t, t_a) \\ &= h_m(t)\cdot s_m(t, t_a) \\ &= \sum_{i=1}^{I}\sum_{p=1}^{P} A_{ip}\phi_{ip}(t)\exp\left[2j\pi f_0 \frac{(m-1)d\sin(\theta_i(t_a))}{c}\right] \\ &\quad \times \exp\left[4j\pi\mu T_d(m-1)\frac{R_{ip}(t_a)}{c}\right] \end{aligned} \tag{25}$$

Thus, the echo of the p-th scatter on the i-th target is vectorized as

$$\tilde{\mathbf{s}}_{ip} = A_{ip}\phi_{ip}(t)\mathbf{a}\left(\theta_i, R_{ip}\right) \tag{26}$$

where $\mathbf{a}\left(\theta_i, R_{ip}\right)$ denotes the receive steering vector, which has the form of

$$\mathbf{a}\left(\theta_i, R_{ip}\right) = \mathbf{d}\left(\theta_i\right) \odot \mathbf{r}\left(R_{ip}\right) \tag{27}$$

$$\mathbf{d}\left(\theta_i\right) = \left[1 \quad e^{j2\pi f_0 \frac{d\sin\theta_i}{c}} \quad \ldots \quad e^{j2\pi f_0 \frac{(M-1)d\sin\theta_i}{c}}\right]^T \tag{28}$$

and

$$\mathbf{r}\left(R_{ip}\right) = \left[1 \quad e^{4j\pi\mu T_d\frac{R_{ip}}{c}} \quad \ldots \quad e^{4j\pi\mu T_d(M-1)\frac{R_{ip}}{c}}\right]^T \tag{29}$$

The time-delay receive array employs time delay across different receive array elements, resulting in range-angle-dependent property of receive steering vector. Utilizing the extra DOFs in angle and range domain, the proposed time-delay receive array can perform beamforming in joint range and angle domain.

Figure.4 compares the receive beampatterns of the traditional phased array and time-delay receive array. It is seen that the beampattern of the traditional phased array is range-invariant, while that of the proposed time-delay receive array is range-angle-dependent. Therefore, targets within the same beam can also be distinguishable in the time-delay receive array if they are associated with different ranges. Besides, the proposed time-delay receive array has the same angular resolution compared with the conventional phased array.

B. JOINT RANGE-ANGLE BEAMFORMING FOR TARGET SEPARATION

In this part, an approach to multiple targets separation is proposed. It is assumed that the slant range and azimuth angle of the interest target is roughly known. In practice, these priori information of target can be obtained from a previous detection mode of radar system.

To extract the echo of the desired target, we need to design a bank of filters that are able to enhance the desired target signal. Without loss of generality, the optimal receive beamforming problem can be expressed as

$$\begin{cases} \min\limits_{\mathbf{w_i}} \mathbf{w_i}^H \mathbf{R}_X \mathbf{w_i} \\ s.t.\mathbf{w_i}^H \mathbf{a}(\theta_i, \mathrm{R}_i) = 1 \end{cases} \tag{30}$$

where $\mathbf{R}_X$ is the covariance matrix of echo. $\mathbf{w_i}$ is the weight vector for i-th target. $\mathbf{a}(\theta_i, R_i)$ is the receive steering vector

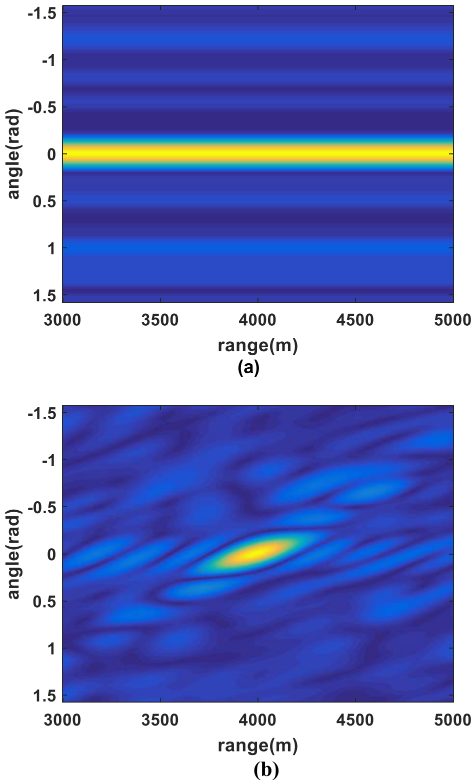

FIGURE 4. Receive beampatterns. (a) Traditional phased array. (b) Time-delay receive array.

of the i-th target. Solving the problem in (30), we can obtain the optimal filter weight vector as

$$\mathbf{w_i} = \frac{\mathbf{R_X^{-1}}\mathbf{a}\left(\theta_i, R_i\right)}{\mathbf{a}^H\left(\theta_i, R_i\right)\mathbf{R_X^{-1}}\mathbf{a}\left(\theta_i, R_i\right)} \tag{31}$$

Actually, the echoes of multiple targets are mixed in the received data matrix. Therefore, the covariance matrix $\mathbf{R}_X$ contains that of the desired target signal, which causes coherent nulling of the desired target signal with (31). To alleviate the coherent nulling problem, we further employ an enhance covariance matrix estimation method as:

$$\hat{\mathbf{R}}_\mathbf{X} = \oiint_{\bar{\Omega}} \frac{\mathbf{a}\left(\theta, R\right)\mathbf{a}^H\left(\theta, R\right)}{\mathbf{a}^H\left(\theta, R\right)\mathbf{R_X^{-1}}\mathbf{a}\left(\theta, R\right)} d\theta dR \tag{32}$$

where $\bar{\Omega}$ is the complement sector of Ω. That is to say, $\bar{\Omega} \cup \Omega$ covers the whole spatial domain, and $\bar{\Omega} \cap \Omega$ is empty. Here is Ω a region where the desired signal is located. With the enhanced covariance matrix estimation method, it is capable of preserving the desired target. Applying the obtained receive weight corresponding to i-th target, we can obtain its echo and suppress the echoes of other adjacent targets. Applying multiple receive weight vectors corresponding to multiple targets, the multi-target echoes can be separated simultaneously. Finally, a well-focused ISAR image of each target can be obtained by performing range alignment and phase compensation.

The processing flow chart can be summarized in Figure 5. In the receiver, time delay is introduced to the received signal by multi-rate sampling. Then, the signal is processed by compensation and receive beamforming to resolve the multiple targets echoes into several single-target parts. A well-focused image of each target can be obtained by performing traditional ISAR imaging algorithm. Thus, the advantages of the proposed time-delay receive array and the corresponding multi-target separation method can be summarized as follows: i) The time-delay receive array can form range-angle-dependent receive beampattern and separate targets in joint range and angle domain. ii) This method can effectively separate multi-target echoes when the signals are submerged by noise after range compression with low SNR as beamforming is independent of target SNR. iii) The proposed method can be applied for imaging of multiple targets with similar motion parameters, which outperforms some traditional multi-target imaging algorithms.

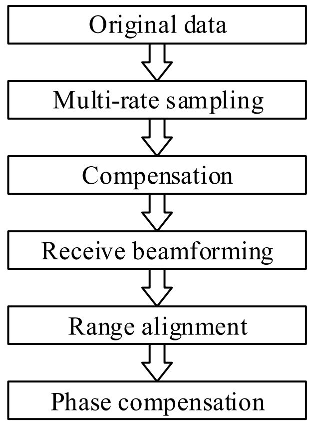

FIGURE 5. Procedure of multiple targets ISAR imaging.

Although the time-delay receive array is compatible with existing radar system, it requires high accuracy of sampling frequency as the sampling difference between adjacent elements is relatively small. Besides, the proposed method increases computation complexity as it includes beamforming procedure for each target.

IV. SIMULATION

In this section, the imaging results of multiple targets in low SNR are given to validate the proposed imaging algorithm. In this simulation, suppose the transmit antenna transmits a wide beam and there are three targets in the wide beam. Build a radar coordinate system with the radar located at $(0°, 0\text{m})$. Target 1, target 2 and target 3 are located at $(5°, 3800\text{m})$, $(-15°, 3800\text{m})$ and $(5°, 4300\text{m})$ respectively as shown in Figure. 6. The system parameters are listed in Table 1. Complex white Gaussian noise is added to returned signal and the signal-to-noise ratio (SNR) is -17dB.

The original echoes are shown in Figure. 7. Due to the low SNR, the echoes are submerged by noise and cannot be separated by range compression. However, the echoes can be separated in equivalent receive frequency domain with time-delay receive array as shown in Figure.8. Subsequently, the signal of target 1 can be extracted from multiple targets echoes by receive beamforming with the beamformer

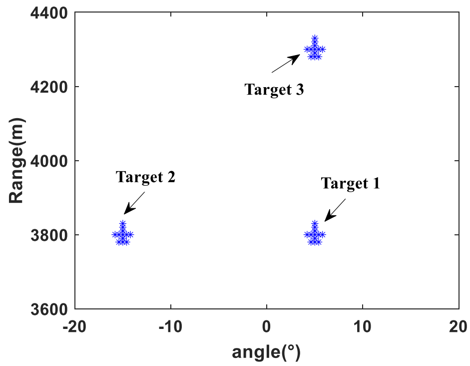

FIGURE 6. Targets position.

TABLE 1. System parameter.

Parameter	Value
Carrier frequency	5.3GHz
Receive element number	12
Element space	0.0283m
PRF	2000Hz
Bandwidth	120MHz
Fast time sampling Frequency	150MHz
Time delay increment	0.8ns
Pulse width	2.5us

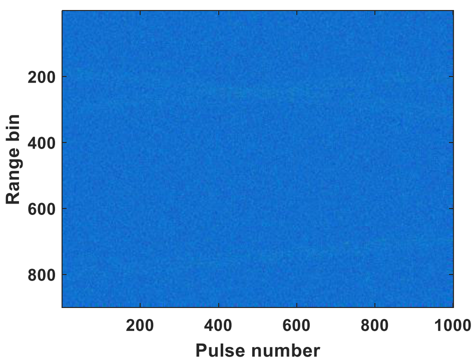

FIGURE 7. Original echo.

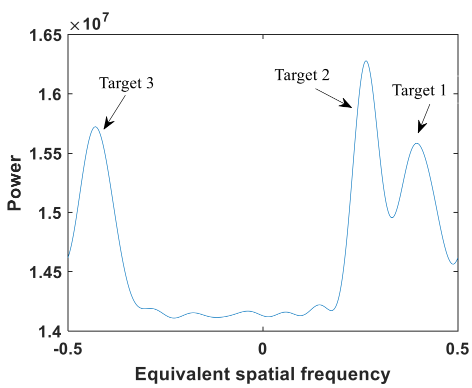

FIGURE 8. Spectrum of multiple targets echo for time-delay receive array.

designed for target 1 as shown in Figure. 9(a). The image of target 1 can be obtained by performing the traditional ISAR imaging algorithm as shown in Figure. 9(b). Similarly, the imaging processing is performed on other targets by substituting the receive beamformer with the one designed for the desired target. So that the imaging results of all targets can be obtained. Figure. 10 and Figure. 11 show the imaging results of target 2 and target 3, respectively. From Figure. 9, Figure. 10 and Figure. 11, it can be seen that the proposed target separation approach has effectively resolved the multiple targets echo into three single-target parts, and the well-focused images can be obtained by subsequent traditional ISAR imaging processing.

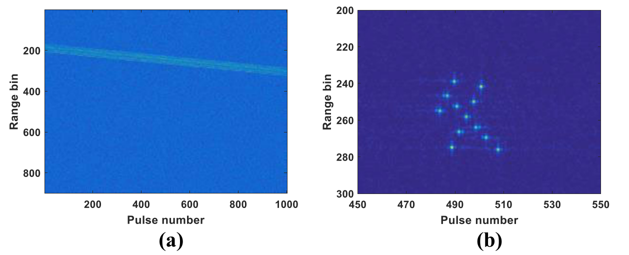

FIGURE 9. Imaging result of target 1. (a) Signal from target 1 after receive beamforming. (b) Image of target 1.

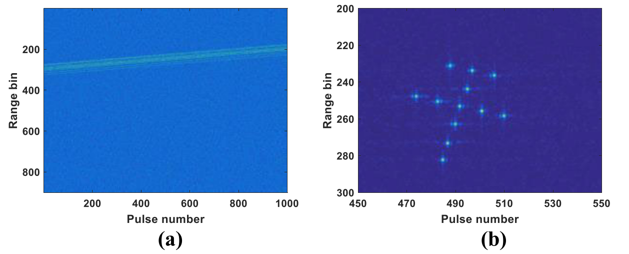

FIGURE 10. Imaging result of target 2. (a) Signal from target 2 after receive beamforming. (b) Image of target 2.

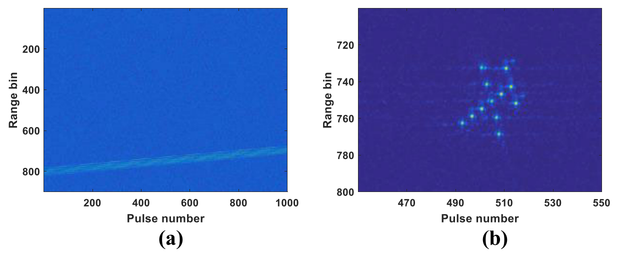

FIGURE 11. Imaging result of target 3. (a) Signal from target 3 after receive beamforming. (b) Image of target 3.

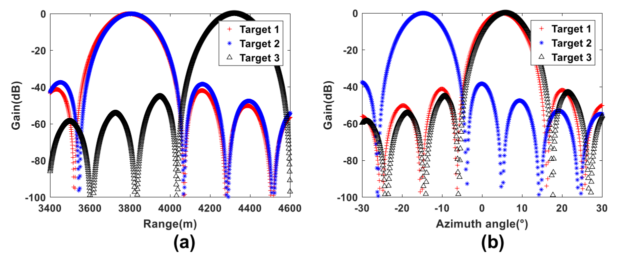

FIGURE 12. Filter response of the receive beamformer. (a) Range. (b)Angle.

Figure. 12(a) and Figure. 12(b) show the filter response of receive beamformer in range and azimuth, respectively. The red line, blue line and black line represent the gain of receive beamformer designed for target 1, target 2 and target 3, respectively. It can be seen from Figure. 12 that the signal

TABLE 2. Imaging performance of targets. Note: PSLR, peak side lobe ratio; ISLR, integral side lobe ratio.

Target number	PSLR of range/dB	PSLR of azimuth/dB	ISLR of range/dB	ISLR of azimuth/dB
1	-14.9	-11.7	-11.8	-10.9
2	-15.5	-11.6	-12.4	-11.3
3	-14.4	-10.1	-12.6	-10.6

TABLE 3. Imaging resolution.

Target number	IRW of range/m	IRW of azimuth/m	Intput SNR/dB	Output SNR/dB
1	1.26	0.50	-17.00	38.14
2	1.24	0.45	-17.00	38.29
3	1.28	0.57	-17.00	37.32

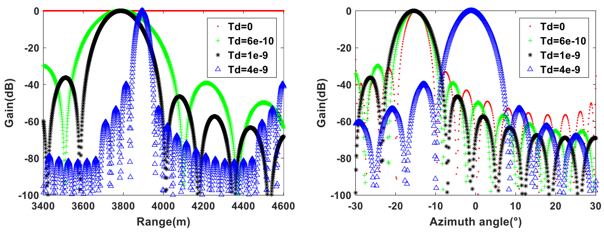

(a) (b)

FIGURE 13. Filter response of receive beamformer with different time delay increment. (a) Range. (b) Angle.

from each target can be separated by receive beamforming in joint range and angle domain.

The peak side lobe ratio (PSLR) of targets and the integral side lobe ratio (ISLR) are listed in Table 2. The resolution of the images and output signal to noise ratio (SNR) are listed in Table 3. It is obvious that target 1, target 2, and target 3 are well focused. The resolution of range is $\rho_r = c/(2B) = 1.25$m in theory. It can be seen from Table 3 that IRW in range are approximate to the theoretical values. In addition, output SNR has increased by 55dB.

Figure. 13(a) and Figure. 13(b) show the filter response of receive beamformer with different time delay increment in range and azimuth. The red line, green line, black line and blue line represent $T_d = 0$, $T_d = 0.6$ns, $T_d = 1$ns and $T_d = 4$ns respectively. From red line, it can be observed that the receive beampattern is only concerned with azimuth angle and independent of range when $T_d = 0$. This is because the array is just a conventional phased-array when time delay increment is 0. It can be observed from Figure. 13(a) that the width of main lobe in range narrows when time delay increment increases, which is conducive to separation of multi-target echoes. However, when the range prior information is not accurate enough, it is difficult to extract the echo of the desired target. Conversely, the width of main lobe in range widens when time delay increment decreases, which is conducive to extract the echo of the desired target when the range prior information is not accurate enough. However, it is not conducive to separate multiple target echoes when multiple targets are close to each other. Besides, the width of main lobe in azimuth angle remain the same when time delay increases. Therefore, it is necessary to choose an appropriate time delay increment.

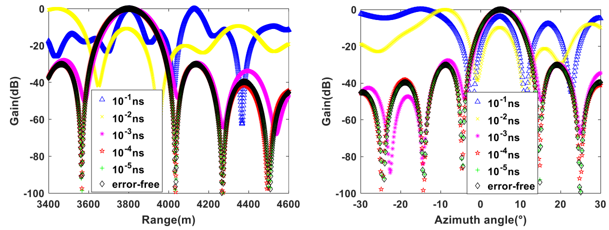

(a) (b)

FIGURE 14. Filter response of the receive beamformer with error. (a) Range. (b) Angle.

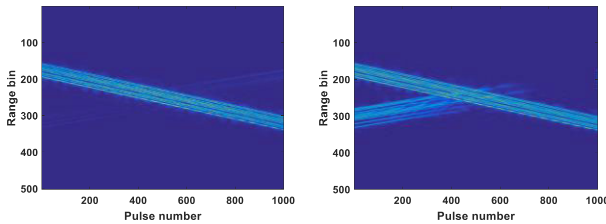

(a) (b)

FIGURE 15. Echo separation performance comparison. (a) Signal from target 1 after separation with the proposed method. (b) Signal from target 1 after separation with the traditional time frequency method.

The proposed method requires high accuracy of sampling frequency as the time-delay increment between adjacent elements is relatively small. In practice, the time delay increment between adjacent elements may be different due to the error of sampling frequency, which affects the performance of multiple targets echoes separation. Figure. 14 shows the filter response of the receive beamformer with time-delay increment error. The blue line, yellow line, pink line, red line, and green line represent that the errors of time-delay increment are in the order of 10^{-1}ns, 10^{-2}ns, 10^{-3}ns, 10^{-4}ns and 10^{-5}ns, respectively. The blank line represents the filter response of the receive beamformer without error. It can be seen from Figure. 14 that multi-target echo cannot be separated effectively when the errors of time-delay increment are greater than 10^{-2}ns.

Afterwards, we compare the imaging performance of the proposed method and the traditional time frequency method as shown in Figure. 15 and Figure. 16. Both of these two methods are based on multi-target separation and independent imaging. The difference is that the former can separate multi-target echoes in equivalent spatial frequency domain by receive beamforming in joint range and angle domain, while the latter can separate multi-target echoes in time frequency domain due to the difference of target motion parameters. Therefore, the traditional time frequency method cannot effectively extract the desired signal from multi-target echoes when the targets have similar velocity or the Doppler ambiguity appears. In this simulation, short-time Fourier transform (STFT) is applied to realizing multi-target echoes separation in time frequency domain.

It can be seen from Figure. 15 that the proposed method can extract the desired signal from multi-target echoes

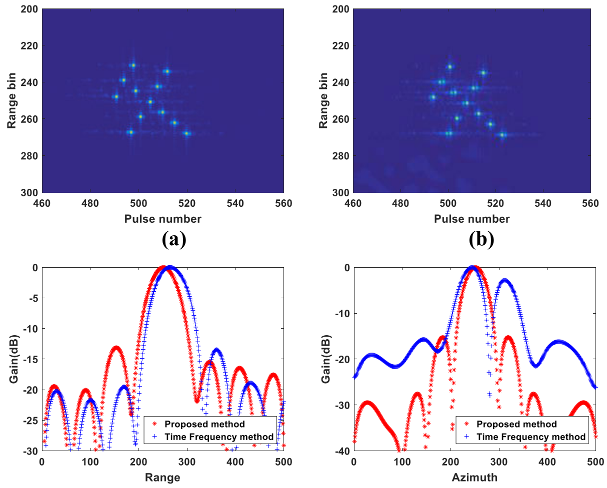

FIGURE 16. Imaging results comparison. (a) Imaging results of target 1 with proposed method. (b) Imaging results of target 1 with the traditional time frequency method. (c) Range profile comparison. (d) Azimuth profile comparison.

more effectively. The SNR of Figure. 16(a) is 65.84dB, while that of Figure. 16(b) is 57.69dB. Figure. 16 (c) and Figure. 16(d) show the range profile comparison and azimuth profile comparison of the same scatter, respectively. It illustrates that the traditional time frequency method has higher PSLR and cannot well focused in azimuth, which is caused by the incomplete echo separation.

V. CONCLUSION

In this paper, a novel time-delay receive system is studied for multiple targets ISAR imaging, realizing multiple targets separation and independent imaging. With this method, multiple targets imaging simultaneous can be achieved in low SNR. Since the receive beampattern of time-delay receive array is range-angle-dependent, the multi-target echoes are distinguishable in the equivalent spatial frequency domain. By exploiting the extra controllable DOFs in range and angle, the time-delay receive array is capable of extracting the desired signal from multi-target echoes. In the sequel, multi-target echoes are resolved into several single-target parts with a series of receive beamformers. Thus, we can obtain the ISAR imaging of each target by performing the traditional imaging method to the reconstructed signal. Evidently, the simulation results have verified the effectiveness of the proposed method. As a future work, we will explore the beamformer design issues for the system.

REFERENCES

[1] C. Ozdemir, *Inverse Synthetic Aperture Radar Imaging With MATLAB Algorithms*. Hoboken, NJ, USA: Wiley, 2012.

[2] V. Chen and H. Ling, *Time-Frequency Transforms for Radar Imaging and Signal Analysis*. Norwood, MA, USA: Artech House, 2001.

[3] C. Noviello, G. Fornaro, P. Braca, and M. Martorella, "ISAR motion compensation based on a new Doppler parameters estimation procedure," in *Proc. IEEE Int. Geosci. Remote Sens. Symp. (IGARSS)*, Milan, Italy, Jul. 2015, pp. 2445–2448, doi: 10.1109/IGARSS.2015.7326304.

[4] C. Noviello, G. Fornaro, M. Martorella, and D. Reale, "A novel approach for motion compensation in ISAR system," in *Proc. EUSAR 10th Eur. Conf. Synth. Aperture Radar*, Berlin, Germany, 2014, pp. 1–4.

[5] M. Xing, R. Wu, Y. Li, and Z. Bao, "New ISAR imaging algorithm based on modified Wigner-Ville distribution," *IET Radar, Sonar Navigat.*, vol. 3, no. 1, pp. 70–80, Feb. 2009, doi: 10.1049/iet-rsn:20080003.

[6] Y. Wang, H. Ling, and V. C. Chen, "ISAR motion compensation via adaptive joint time-frequency technique," *IEEE Trans. Aerosp. Electron. Syst.*, vol. 34, no. 2, pp. 670–677, Apr. 1998, doi: 10.1109/7.670350.

[7] C. Jian-Wen, J. Ke-Peng, and W. Jun, "ISAR imaging of multiple targets based on FrFT-CLEAN," in *Proc. Int. Conf. Microw. Technol. Comput. Electromagn. (ICMTCE)*, Beijing, China, 2009, pp. 137–140, doi: 10.1049/cp.2009.1294.

[8] Y. Li, Y. Fu, X. Li, and L. Le-Wei, "ISAR imaging of multiple targets using particle imaging of multiple targets using particle swarm optimisation–daptive joint time frequency approach," *IET Signal Process.*, vol. 4, no. 4, pp. 343–351, Aug. 2010, doi: 10.1049/iet-spr.2009.0046.

[9] S. H. Park, K. K. Park, J. H. Jung, H. T. Kim, and k. T. Kim, "ISAR imaging of multiple targets using edge detection and Hough transform," *J. Electromagn. Waves Appl.*, vol. 22, nos. 2–3, pp. 365–373, 2008.

[10] S.-H. Park, H.-T. Kim, and K.-T. Kim, "Segmentation of ISAR images of targets moving in formation," *IEEE Trans. Geosci. Remote Sens.*, vol. 48, no. 4, pp. 2099–2108, Apr. 2010, doi: 10.1109/TGRS.2009.2033266.

[11] X. Bai, F. Zhou, M. Xing, and Z. Bao, "A novel method for imaging of group targets moving in a formation," *IEEE Trans. Geosci. Remote Sens.*, vol. 50, no. 1, pp. 221–231, Jan. 2012, doi: 10.1109/TGRS.2011.2160185.

[12] M. Martorella, E. Giusti, F. Berizzi, A. Bacci, and E. D. Mese, "ISAR based techniques for refocusing non-cooperative targets in SAR images," *IET Radar, Sonar Navigat.*, vol. 6, no. 5, pp. 332–340, Jun. 2012, doi: 10.1049/iet-rsn.2011.0310.

[13] J. Chen, H. Xiao, Z. Song, and H. Fan, "Imaging targets moving in formation using parametric compensation," *EURASIP J. Adv. Signal Process.*, vol. 2014, no. 1, pp. 1–8, Dec. 2014.

[14] P. Antonik, M. C. Wicks, H. D. Griffiths, and C. J. Baker, "Range-dependent beamforming using element level waveform diversity," in *Proc. Int. Waveform Diversity Design Conf.*, Lihue, HI, USA, Jan. 2006, pp. 1–6, doi: 10.1109/WDD.2006.8321488.

[15] P. Antonik, M. C. Wicks, H. D. Griffiths, and C. J. Baker, "Frequency diverse array radars," in *Proc. IEEE Conf. Radar*, Verona, NY, USA, Apr. 2006, p. 3, doi: 10.1109/RADAR.2006.1631800.

[16] M. Secmen, S. Demir, A. Hizal, and T. Eker, "Frequency diverse array antenna with periodic time modulated pattern in range and angle," in *Proc. IEEE Radar Conf.*, Boston, MA, USA, Apr. 2007, pp. 427–430, doi: 10.1109/RADAR.2007.374254.

[17] W.-Q. Wang, "Range-angle dependent transmit beampattern synthesis for linear frequency diverse arrays," *IEEE Trans. Antennas Propag.*, vol. 61, no. 8, pp. 4073–4081, Aug. 2013, doi: 10.1109/TAP.2013.2260515.

[18] P. F. Sammartino, C. J. Baker, and H. D. Griffiths, "Frequency diverse MIMO techniques for radar," *IEEE Trans. Aerosp. Electron. Syst.*, vol. 49, no. 1, pp. 201–222, Jan. 2013, doi: 10.1109/TAES.2013.6404099.

[19] J. Xu, G. Liao, S. Zhu, L. Huang, and H. C. So, "Joint range and angle estimation using MIMO radar with frequency diverse array," *IEEE Trans. Signal Process.*, vol. 63, no. 13, pp. 3396–3410, Jul. 2015, doi: 10.1109/TSP.2015.2422680.

[20] J. Xu, G. Liao, Y. Zhang, H. Ji, and L. Huang, "An adaptive range-angle-Doppler processing approach for FDA-MIMO radar using three-dimensional localization," *IEEE J. Sel. Topics Signal Process.*, vol. 11, no. 2, pp. 309–320, Mar. 2017, doi: 10.1109/JSTSP.2016.2615269.

[21] J. Xu, S. Zhu, and G. Liao, "Range ambiguous clutter suppression for airborne FDA-STAP radar," *IEEE J. Sel. Topics Signal Process.*, vol. 9, no. 8, pp. 1620–1631, Dec. 2015, doi: 10.1109/JSTSP.2015.2465353.

[22] C. Wang, J. Xu, G. Liao, X. Xu, and Y. Zhang, "A range ambiguity resolution approach for high-resolution and wide-swath SAR imaging using frequency diverse array," *IEEE J. Sel. Topics Signal Process.*, vol. 11, no. 2, pp. 336–346, Mar. 2017, doi: 10.1109/JSTSP.2016.2605064.

MENGDI ZHANG was born in Xianyang, China, in 1994. She received the B.S. degree in electronics engineering from Xidian University, Xi'an, in 2016, where she is currently pursuing the Ph.D. degree with the National Laboratory of Radar Signal Processing. Her research interests include frequency diverse array radar systems, MIMO radar signal processing, and SARs.

GUISHENG LIAO (Senior Member, IEEE) was born in Guilin, China, in 1963. He received the B.S. degree from Guangxi University, Guangxi, China, in 1985, and the M.S. and Ph.D. degrees from Xidian University, Xi'an, China, in 1990 and 1992, respectively.

From 1999 to 2000, he was a Senior Visiting Scholar with The Chinese University of Hong Kong, Hong Kong. Since 2006, he has served as the panelists for the medium and long term development plan in high-resolution and remote sensing systems. Since 2007, he has been the Lead of Yangtze River Scholars Innovative Team and devoted in advanced techniques in signal and information processing. Since 2009, he has been the Evaluation Expert of the International Cooperation Project of Ministry of Science and Technology in China. He is currently a Yangtze River Scholars Distinguished Professor with the National Laboratory of Radar Signal Processing and serves as the Dean of the School of Electronics Engineering, Xidian University. His research interests include array signal processing, space-time adaptive processing, radar waveform design, airborne/space surveillance, and warning radar systems.

JINGWEI XU (Member, IEEE) was born in Shandong, China. He received the B.S. degree in electronics engineering and the Ph.D. degree in signal and information processing from Xidian University, China, in 2010 and 2015, respectively.

From 2015 to 2017, he was a Lecturer at the National Laboratory of Radar Signal Processing, Xidian University. From 2017 to 2019, he was a Postdoctoral Fellow of The City University of Hong Kong, through the "Hong Kong Scholar Program". He is currently an Associate Professor with the School of Electronics Engineering, Xidian University. His research interests include waveform diverse array radars, multi-sensor array signal processing, space-time adaptive processing, and multiple-input multiple-output radars.

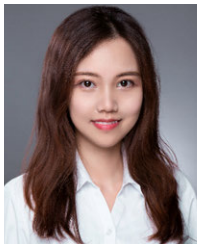

LAN LAN (Member, IEEE) was born in Xi'an, China, in 1993. She received the B.S. degree in electronics engineering and the Ph.D. degree in signal and information processing from Xidian University, Xi'an, in 2015 and 2020, respectively.

She was a Visiting Ph.D. Student with the University of Naples Federico II, Naples, Italy, from July 2019 to July 2020. She has been a Tenure-Track Associated Professor with the National Laboratory of Radar Signal Processing, Xidian University, since August 2020. Her research interests include frequency diverse array radar systems, MIMO radar signal processing, target detection, and the ECCM. She was a recipient of the Excellent Paper Award from the CIE International Conference on Radars in 2016.

KA DENG received the B.E. degree from Xidian University in 2010 and the Ph.D. degree from Tsinghua University in 2017. He is an Assistant Professor with the Shenzhen Institutes of Advanced Technology (SIAT), Chinese Academy of Sciences (CAS). His current research interests include robotics and engineering problems in wearable devices, laboratory automation, and walking locomotion.